JOURNAL OF GUIDANCE, CONTROL, AND DYNAMICS
Vol. 17, No. 2, March–April 1994

Broadband Control of Flexible Structures Using Statistical Energy Analysis Concepts

Douglas G. MacMartin
National Research Council of Canada, Ottawa, Ontario, K1A-0R6 Canada
and
Steven R. Hall
Massachusetts Institute of Technology, Cambridge, Massachusetts 02139

An approach is described for designing optimal broadband controllers for flexible structures with collocated sensors and actuators. The statistical energy analysis assumptions of equipartition and incoherence, together with conservation of energy, are used to express the average value of a global $\mathcal{H}_2$ performance metric in terms of the power dissipation of the compensator. This power dissipation can be represented using a dereverberated model, which is an experimentally determined local structural model that ignores the effect of the reverberant field. Minimizing the resulting cost yields controllers with good performance that are guaranteed to be stabilizing. The approach is demonstrated experimentally on the Massachusetts Institute of Technology Space Engineering Research Center interferometer testbed. This approach achieved a performance reduction that was approximately 30% greater than that obtained with a constant gain "rate feedback" approach.

I. Introduction

ACTIVE control of lightly damped, modally dense structures is difficult due to the parametric uncertainty that is inherent in any model of such a structure. The first few modes of the structure can usually be modeled with sufficient accuracy for many state space control design techniques. However, it may be necessary to have some control authority over many more modes of the structure. This need might be due to stringent performance requirements,[1] a need to control relatively high frequency modes that couple into audible acoustic modes,[2] or a requirement to add active damping to structural modes in the roll-off region of a high authority controller.[3] This paper investigates the design of optimal compensators to achieve these goals. A major aspect of this investigation is the modeling of the uncertain structure in this frequency region to facilitate the control design.

A broadband controller that affects many modes of the structure need only be designed for the high frequency region in which modal uncertainty is significant. Robustness is guaranteed by taking advantage of the positivity between collocated and dual sensors and actuators, where duality implies that the product of the sensed and actuated variables is proportional to the power flow into the structure. At low frequencies where a good model is available, a high authority controller (HAC) can be designed using noncollocated, multiple-input multiple-output (MIMO) loops, and the two controllers can be combined in a high authority control/low authority control (HAC/LAC), law authority controller, architecture.[3] The damping of LAC could be provided passively. However, active damping can be more easily tuned to target relatively narrow frequency bands. Furthermore, if the hardware required for an active approach is already present to implement the HAC, there

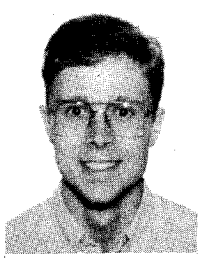

Douglas MacMartin received his B.A.Sc. in the Aerospace option of Engineering Science from the University of Toronto in 1987, and his S.M. and Ph.D. in Aeronautics and Astronautics from the Massachusetts Institute of Technology in 1990 and 1992, respectively. He is now with the Aeroacoustics Facility of the Institute for Aerospace Research, at the National Research Council of Canada. His current research interests are in active noise and vibration control. He is a Member of AIAA and IEEE.

Steven R. Hall received his S.B., S.M., and Sc.D. degrees from the Massachusetts Institute of Technology, Department of Aeronautics and Astronautics, in 1980, 1982, and 1985, respectively. Since 1985, he has been on the faculty at MIT., where he is currently Associate Professor of Aeronautics and Astronautics. His research interests include active control of flexible structures and the control of helicopter vibration and rotor dynamics. He is a Senior Member of AIAA, and a member of IEEE and the American Helicopter Society.

Received Dec. 2, 1992; revision received July 21, 1993; accepted for publication July 28, 1993.

may be very little additional weight penalty associated with the LAC.

Because of the number of modes in the bandwidth of these problems and the uncertainty in their frequencies and mode shapes, it may be useful to model only some statistical aspects of the response, rather than attempting to model the detailed modal behavior. One field of research that uses a stochastic approach to the modeling of flexible structures is statistical energy analysis (SEA).[4,5] To obtain accurate response estimates using minimal information, SEA makes use of conservation of energy and also assumes incoherence and equipartition. Incoherence requires that different modal amplitudes be uncorrelated, and equipartition requires that modes closely spaced in frequency have similar energy. These properties have been shown to hold for the average over uncertainty of the state space covariance.[6] SEA also makes use of an average, or dereverberated, input mobility to make power flow predictions for uncertain structures.

Previous research with a dereverberated model,[7] and with related wave-based models[8,9] has shown that an impedance matching control design approach can yield greater damping than the collocated rate feedback typically used for the LAC. Both $\mathcal{H}_2$[9] and $\mathcal{H}_\infty$[7] optimizations of the power flow have been used. The $\mathcal{H}_2$ approach does not guarantee closed-loop stability when implemented on the actual structure, and the $\mathcal{H}_\infty$ approach does not minimize the actual global $\mathcal{H}_2$ cost functional. Neither approach incorporates sufficient information about the structure into the control design process.

The structural modeling principles used in this paper are strongly motivated by SEA. A dereverberated model is used to describe the local structural properties at a collocated and dual actuator/sensor pair. This model can be obtained directly from experimental data. The structure is assumed to be random, and hence the equipartition and incoherence properties hold. The expected value of the desired global quadratic cost can then be computed in terms of the local structural properties. Note that the cost is averaged over both the driving noise and the uncertainty in the structure. This cost can be expressed as a mixed $\mathcal{H}_2/\mathcal{H}_\infty$ cost functional of the power flow properties and can be evaluated using the state space representation of the dereverberated structural model and of the compensator. The compensator that minimizes this cost can be obtained from a numerical optimization. An $\mathcal{H}_\infty$ constraint is incorporated, similar to that in Ref. 7, which guarantees that the optimal compensator will be positive real, and hence stabilizing for any uncertainty in the structure.

II. Local Modeling

The purpose of the LAC is to add damping in a frequency region in which the structural modes are uncertain. A detailed modal model is therefore inappropriate, because much of the information it contains is meaningless. For sufficiently large uncertainty, the phase of any noncollocated transfer function is completely unknown. However, there is some phase information in the transfer

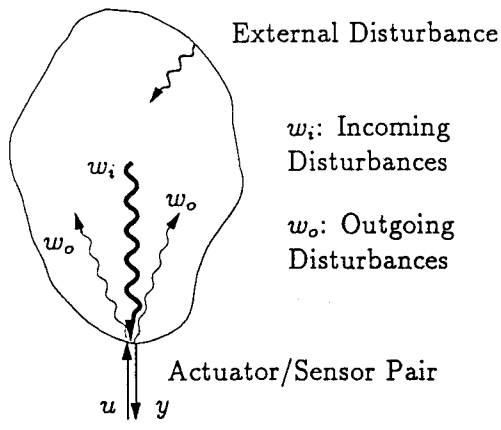

Fig. 1 Arbitrary structure.

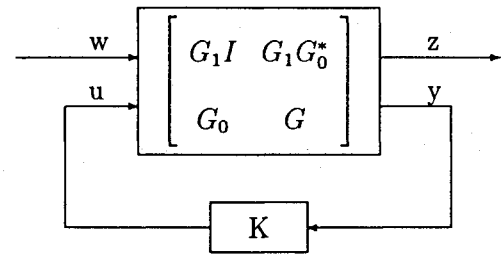

Fig. 2 Power flow model with control u, compensator K, output y, and normalized incoming and outgoing disturbances w and z.

function between collocated and dual actuators and sensors. To develop an appropriate model for such a transfer function, consider an arbitrary structure as shown in Fig. 1, from Ref. 7. Incoming disturbances w_i propagate toward the actuator/sensor location and are partially dissipated and partially reflected back into the structure as outgoing disturbances w_o. To maximize dissipation, only the "local" structural dynamics that describe the relationship between the inputs u and w_i and the outputs y and w_o must be known. The scale length associated with the term local is related to the wavelength of the disturbances being considered. The details of how w_o propagates throughout the structure and returns as another incoming disturbance w_i are uncertain. Rather than including this propagation in the model, it will be accounted for later using conservation of energy.

The local dynamics can be modeled using the dereverberation approach from SEA.[7] The response due to the actuator can be divided into a direct field that is due to the local dynamics, and a reverberant field that is created by reflections from other parts of the structure. The dereverberated model includes only the effects of the direct field. There are a variety of equivalent interpretations of this model. It appears in Ref. 5 as the average of the logarithmic magnitude of the mobility over frequency bands containing many modes. It is also equivalent to the limiting transfer function obtained as the damping is increased,[4,10] since the reverberant field is eliminated as the damping becomes critical. This leaves only the effects of the direct field, and hence yields the dereverberated mobility. The reverberant field can also be eliminated by considering the transfer function of the infinitely extended system, allowing the dereverberated mobility to be computed from a wave model.[11] A final interpretation is as the large uncertainty limit of averaging the driving point mobility over uncertainty.[12]

Given the experimentally measured reverberant transfer function $G_{\exp}(s)$, the dereverberated transfer function $G(s)$ can be obtained by taking an average of the logarithmic magnitude. That is, $G(s)$ minimizes a cost functional of the form

$$\int_0^\infty (\log|G_{\exp}| - \log|G|)^2 \, \mathrm{d}(\log\omega) \tag{1}$$

Since complex poles are associated with oscillation, or reverberation, the dereverberated transfer function can be described using only real poles and zeroes. Hence, write that

$$G(s) = k \frac{\prod_{i=1}^{n_z} (s + b_i)}{\prod_{i=1}^{n_p} (s + a_i)} \tag{2}$$

where $a_i \geq 0$, $i = 1,\ldots, n_p$, $b_i \geq 0$, $i = 1,\ldots, n_z$, and n_z is either n_p or $n_p - 1$. Minimizing the cost in Eq. (1) with $G(s)$ constrained to be of the form in Eq. (2) gives the desired transfer function. The gradients can be computed analytically, and the minimization performed using a quasi-Newton search routine. The number of poles used to describe the dereverberated transfer function can be increased until there is no significant decrease in the cost. Usually,

only a few poles are required. A typical comparison of the dereverberated and measured transfer functions is shown in Fig. 6.

Once the dereverberated driving point mobility G for the system has been obtained, the power properties of the driving point can be represented in state space for control design, as in Ref. 7. Find G_0 stable and minimum phase and G_1 inner (or all-pass) such that $G_0G_0^* = G + G^*$ and $G_1G_0^*$ is stable. State-space representations for these transfer functions can be obtained from the state space representation of G.[7] The resulting control problem can now be formulated as a standard two-input two-output problem, as shown in Fig. 2. The inputs are the control u and the disturbance w, normalized so that w^*w is the incoming power. The outputs are the sensor signal y and a cost variable z, defined so that z^*z is the power reflected back into the structure as a function of frequency. This figure describes the two-input, two-output actuator/sensor location in Fig. 1; w and z here correspond to the incoming and outgoing waves w_i and w_o.

The transfer function from w to z is given by the lower linear fractional transformation (LFT)

$$H(s) \triangleq \frac{z(s)}{w(s)} = G_1 I + G_1 G_0^* K (I - GK)^{-1} G_0 \tag{3}$$

Because of the normalization of the disturbance w, H^*H is the fraction of the incoming power reflected back into the structure from the control system, and $(I - H^*H)$ is the fraction dissipated by the controller. The transfer function H is the generalization of the reflection coefficient in a wave model to an arbitrary structure. In open loop, $H = I$ and $I - H^*H = 0$.

The compensator that dissipates the most power, frequency by frequency, is the impedance matching control law[7]

$$u = \frac{1}{G^T(-s)} y \tag{4}$$

which yields $H = 0$ and $I - H^*H = I$. This impedance matching solution is only appropriate if the dereverberated transfer function is used, rather than the full reverberant transfer function.[11] The impedance match of the reverberant transfer function may make the structure less damped, so that more power is added to the structure by the disturbance, and hence more power is available to be dissipated. The problem is that the correct performance metric is not just the power input to the structure from the control, but the total power input from both the control and the external disturbances. However, if the structure is sufficiently uncertain, then the control will be uncorrelated with the disturbance, and the disturbance input power can be ignored when determining the optimal control law. For this case, the control will also be uncorrelated with the reverberant field at the control location, and hence only the dereverberated transfer function should be used.

The compensator in Eq. (4) is noncausal (or unstable) unless $G(s)$ is a constant, and a stable, causal approximation must be found. The cost functional derived in the next section implicitly describes the relative importance of matching the magnitude and phase of the noncausal impedance match and the relative importance of different frequency regions.

III. Performance Metric for Uncertain Structures

The average value of a global $\mathcal{H}_2$ performance metric can be described in terms of the local structural information by taking advantage of the properties of parametrically uncertain systems. In particular, the average covariance satisfies the SEA assumptions of equipartition and incoherence,[6] as well as conservation of energy.

Incoherence implies that the amplitudes of different modes are uncorrelated. For a given structure, this behavior will not occur unless the disturbances are spatially distributed. However, incoherence also results from averaging the covariance over an uncertainty distribution.[6] Equipartition requires that all modes within a given subsystem and within the same frequency band have the same energy. This characteristic will not usually be true unless the disturbances are both spatially distributed and broadband. However, for the purposes of manipulating the average $\mathcal{H}_2$ cost, it is sufficient that equipartition be satisfied for each individual mode. That is, the kinetic and potential energy of each mode must be equal, but the energy of one mode need not be equal to that of any other. This behavior holds for the average energy of structures with uncertain natural frequencies.[6] From a wave perspective, there is a single assumption corresponding to equipartition and incoherence, which is that of a "diffuse" field.[4] This means that at any point within the system, the waves coming from all directions are uncorrelated, and have equal intensities.

Let $\langle \cdot \rangle_w$ denote the expected value of $(\cdot)$ with respect to the noise w, and $\langle \cdot \rangle$ the expected value with respect to both the noise and the uncertainty in the structure. The global $\mathcal{H}_2$ cost can be written as $\sqrt{\langle z^T z \rangle_w}$, where $z(t)$ is a vector that depends on the deflections and velocities of the structure. Expanding the performance vector in terms of modes, with modal amplitudes $\psi_n(t)$, gives

$$z(t) = \sum_{n=0}^{\infty} c_n \psi_n(t) + \sum_{n=0}^{\infty} c_n' \dot{\psi}_n(t) \tag{5}$$

for appropriately defined coefficients c_n and c_n'. For the average covariance over uncertainty, equipartition holds for each mode, so the modes can be normalized such that the energy of mode n is $E_n = \frac{1}{2}\langle \psi_n^2 \rangle = \frac{1}{2}\langle \dot{\psi}_n^2 \rangle / \omega_n^2$. Using incoherence, the average mean-square value of z over both the uncertainty and the noise can be expressed as a sum over the average modal energies

$$\langle z^T z \rangle = 2 \sum_{n=0}^{\infty} E_n (c_n^T c_n + \omega_n^2 c_n'^T c_n') \tag{6}$$

A similar relationship is observed in SEA (Ref. 4, p. 119).

For a modally dense structure, the sum in Eq. (6) can be approximated by an integral of the form

$$J = \langle z^T z \rangle \cong \int_{-\infty}^{\infty} C(\omega) E(\omega) \, d\omega \tag{7}$$

The function $E(\omega)$ is the average energy in the structure per unit bandwidth. The performance weighting function $C(\omega)$ in Eq. (7) is obtained by averaging $c_n^T c_n + \omega_n^2 c_n'^T c_n'$ over the modes in each frequency region, and multiplying by the modal density. The approximation in Eq. (7) is valid above the Schroeder cutoff frequency,[13] where the modal spacing is equal to the half power bandwidth of each mode. With modal frequency uncertainty, the average system has a smoother transfer function, and hence a lower Schroeder cutoff frequency. For the limiting case that yields the dereverberated mobility as the average transfer function, Eq. (7) holds at all frequencies.

Assuming a diffuse field (or equivalently, assuming equipartition and incoherence), all waves have equal intensity proportional to the structural energy.[4] Thus the power flowing toward the actuator is proportional to the total energy in the structure. Using the results of Sec. II yields

$$\Pi_{\text{diss}}(\omega) = [I - H(j\omega)^* H(j\omega)] E(\omega) \tag{8}$$

The power dissipated by the controller, Π_{diss}, can be determined from conservation of energy

$$\omega \eta E + \Pi_{\text{diss}} = \Pi_{\text{in}} \tag{9}$$

The first term is the power dissipation within the structure, which is proportional to the average structural energy E. The loss factor η is often poorly known, but is sufficiently small for many applications that it can be assumed to be negligible.

The power input from external disturbance sources $\Pi_{\text{in}}(\omega)$ in Eq. (9) can be estimated or measured reasonably well for most sys-

tems. If the disturbances are specified by the power spectral density $V(\omega)$ of a force input, then the power can be determined by using the dereverberated mobility G_d at the disturbance source, since the reverberant field does not contribute to the mean input power.[4]

$$\Pi_{in} = (G_d + G_d^*)V \tag{10}$$

The total power input is the sum of the power from each disturbance source. If the dereverberated mobility at the disturbance cannot be measured or estimated, or if the disturbances are unknown, Π_{in} can be obtained by measuring the spatially averaged modal energy, and using Eq. (9) with $\Pi_{diss} = 0$.

Eqs. (8) and (9) can be solved for the structural energy, giving

$$E(\omega) = \frac{\Pi_{in}(\omega)}{(\gamma^2 I - H^*H)} \tag{11}$$

where $\gamma = \sqrt{1 + \omega\eta}$. Eq. (11) is valid provided that $\|H\|_\infty < \gamma$, so that the required inverse exists. Otherwise, the power added by the control exceeds that dissipated by the damping, and the cost is infinite. The damping parameter γ and the reflection coefficient H are functions of frequency, and are not indicated as such for brevity.

From Eqs. (7) and (11), the total cost over all frequencies is

$$J = \int_{-\infty}^{\infty} \frac{1}{\gamma^2} \frac{C(\omega)\Pi_{in}(\omega)}{(I - \gamma^{-2}H^*H)}\, d\omega \tag{12}$$

The maximum possible power is dissipated by a non-causal compensator, which yields $H = 0$, and a closed-loop cost of

$$J_{min} = \int_{-\infty}^{\infty} \frac{1}{\gamma^2} C(\omega)\Pi_{in}(\omega)\, d\omega \tag{13}$$

This expression provides an alternate approach for obtaining the weighting functions. Rather than separately computing the effect of the disturbance on the structural energy, given by $\Pi_{in}(\omega)$, and the effect of the structural energy on the quadratic cost, given by $C(\omega)$, the product of the weightings can be computed directly. The integrand of Eq. (13) is the minimum achievable quadratic performance at each frequency, obtained if the structure is critically damped. The weighting function $W(j\omega)$ satisfying $W(j\omega)^*W(j\omega) = \gamma^{-2}C(\omega)\Pi_{in}(\omega)$ can therefore be computed by measuring the transfer function from disturbance to performance, and obtaining the damped transfer function using the same algorithm as the computation of the dereverberated transfer functions. Shaping filters that give the power spectral density of the disturbance from white noise should be included in the weighting.

Subtracting the minimum achievable cost in Eq. (13) from the total cost does not change the minimization problem, but yields a better conditioned optimization problem and elucidates certain features of the cost. Therefore, redefine the cost to be

$$J = \int_{-\infty}^{\infty} C(\omega)\Pi_{in}(\omega) \frac{\gamma^{-2}H^*H}{I - \gamma^{-2}H^*H}\, d\omega \tag{14}$$

The compensator that minimizes this cost also minimizes the average, with respect to uncertainty, of the global $\mathcal{H}_2$ performance metric. The knowledge that the structure approximately conserves energy is preserved.

This cost can be compared with those of previous optimal impedance matching approaches. Given the spectrum Φ_{dd} of the incoming waves, the $\mathcal{H}_2$ cost of Miller et al.[9] is

$$J_{\mathcal{H}_2} = \int_{-\infty}^{\infty} \mathrm{tr}\{\Phi_{dd}(\omega) H^*H\}\, d\omega \tag{15}$$

The unweighted $\mathcal{H}_\infty$ cost of MacMartin and Hall[7] is $J_{\mathcal{H}_\infty} = \|H\|_\infty$.

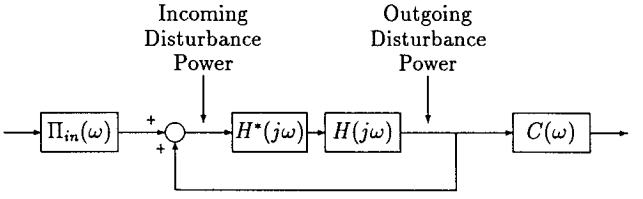

Fig. 3 Block diagram representation of cost.

The integrand of the cost in Eq. (14) can be represented in block diagram form as shown in Fig. 3. The $\mathcal{H}_2$ minimization of power flow in Eq. (15) is equivalent to the block diagram without the feedback loop. The main difficulty with the $\mathcal{H}_2$ approach was that it gave no guarantee of stability, since there is nothing in the formulation that prevents the controller from adding energy to the structure at certain frequencies. The presence of the feedback loop in the block diagram representation accounts for the fact that the structure conserves energy; that is, that any energy imparted to the structure at some frequency will eventually return to the actuator location. Thus the disturbance power spectrum that reaches the actuator is the sum of the external disturbance power and the outgoing disturbance power, as indicated in Fig. 4.

With reference to the structure in Fig. 1, this result corresponds to ignoring the details of how the outgoing disturbance w_o propagates and returns as another incoming disturbance w_i, but retaining the fact that it does return. The phase of the returning disturbance is assumed unknown, but for light damping, the energy is the same as that in w_o. All of the uncertainty in the structure has therefore been represented in terms of a single uncertainty with unit magnitude and unknown phase, which leads to an $\mathcal{H}_2/\mathcal{H}_\infty$ interpretation of the cost in Eq. (14).

This cost functional is strongly related to the $\mathcal{H}_2/\mathcal{H}_\infty$ approach taken in Ref. 14, and also has an interpretation in terms of a Stackelberg nonzero sum dynamic differential game.[15] With unity weightings, the cost is also the average $\mathcal{H}_2$ cost of the system $(I - H\Delta)^{-1}H$ where the uncertainty Δ has known magnitude but unknown phase.[11] This is analogous to the interpretation of the entropy as the average $\mathcal{H}_2$ cost over a set of uncertainty with bounded magnitude and unknown phase [Ref. 16, p. 114].

Both $\Pi_{in}(\omega)$ and $C(\omega)$ in Eq. (14) are purely real functions of frequency, and can thus be factored as $\Pi_{in}(\omega) = \Pi_+^* \Pi_+$ and $C(\omega) = C_+^* C_+$, where $\Pi_+(j\omega)$ and $C_+(j\omega)$ are both stable. Define $H_0 = \sqrt{2\pi}\gamma^{-2} C_+ H \Pi_+$, and $H_1 = H$. Then the combined $\mathcal{H}_2/\mathcal{H}_\infty$ cost functional considered here can be defined more formally as follows.

Definition 1. Consider a system $\hat{H}(s) = [H_0(s)\ H_1(s)]$ and a positive number $\gamma \in \mathcal{R}$, with $H_0 \in \mathcal{H}_2$, $H_1 \in \mathcal{H}_\infty$, and $\|H_1\|_\infty < \gamma$. Then the cost $L(\hat{H}, \gamma)$ is defined by

$$L(\hat{H}, \gamma) \triangleq \frac{1}{2\pi} \int_{-\infty}^{\infty} \mathrm{tr}\{ (I - \gamma^{-2} H_1 H_1^*)^{-1} H_0 H_0^* \}\, d\omega \tag{16}$$

The expected value of the global $\mathcal{H}_2$ performance metric for an undamped structure is minimized by minimizing $L([\sqrt{2\pi} C_+ H \Pi_+\ H], 1)$. Further properties on this cost functional can be found in Ref. 15.

IV. Optimization of Performance

The compensator that minimizes $L(\hat{H}, \gamma)$ will guarantee that $\|H_1\|_\infty < \gamma$, so that between the controller and the internal dissipation, power is dissipated at all frequencies, and thus the closed-loop system is stable. A numerical optimization approach for obtaining the optimal compensator has been used, since there is no known closed form solution. This approach is based on a state space evaluation of the cost, and the derivatives of this cost with respect to the parameters of a fixed-order compensator. A quasi-Newton algorithm was used in this research.

Given the state-space representation of the compensator and the dereverberated mobility, the state-space representation of H can be obtained from the LFT in Eq. (3). The state-space representation of $\hat{H}(s) = [H_0(s)\ H_1(s)] = [\sqrt{2\pi}C_+ H \Pi_+\ H]$ can be obtained from those of H and the weightings $C(\omega)$ and $\Pi_{in}(\omega)$. The cost can then be evaluated based on the following theorem from Refs. 11 and 15. Consider a state-space representation for a proper system $\hat{H} = [H_0\ H_1]$

$$\hat{H}(s) = C(sI-A)^{-1}[B_0\ B_1] + [0\ D] \tag{17}$$

$$\sim \left[\begin{array}{c|cc} A & B_0 & B_1 \\ \hline C & 0 & D \end{array}\right] \tag{18}$$

and define

$$\begin{aligned} Z &= (I-\gamma^{-2}DD^T)^{-1} \\ W &= (I-\gamma^{-2}D^TD)^{-1} \\ \bar{A} &= A+\gamma^{-2}B_1D^TZC \end{aligned} \tag{19}$$

If a nonzero term D_0 were included in Eq. (18), then $H_0 \notin \mathcal{H}_2$ and hence $L(\hat{H}, \gamma)$ would not exist. In the case $D = 0$, these equations simplify considerably.

Theorem 2. Let $\hat{H} = [H_0\ H_1]$ be given by Eq. (18) Z, W, and $\bar{A}$ given by Eq. (19), $\gamma \in \mathcal{R}$, and $\|H_1\|_\infty < \gamma$. Then

$$L(\hat{H}, \gamma) = \text{tr}\,\{C^TZCQ\} \tag{20}$$

where Y and Q satisfy $(\bar{A} + YC^TZC)$ stable and

$$\bar{A}Y + Y\bar{A}^T + YC^TZCY + \gamma^{-2}B_1WB_1^T = 0 \tag{21}$$

$$(\bar{A} + YC^TZC)Q + Q(\bar{A} + YC^TZC)^T + B_0B_0^T = 0 \tag{22}$$

Proof: Both Z and W exist since $\|H_1\|_\infty < \gamma$. Also, $\exists\ M \in \mathcal{H}_\infty$ given by

$$M^*M = H_0^*(I-\gamma^{-2}H_1H_1^*)^{-1}H_0 \tag{23}$$

A minimal state-space representation for M^*M can be obtained by straightforward algebraic manipulations[11]

$$M^*M \sim \left[\begin{array}{cc|c} \bar{A} & \gamma^{-2}B_1WB_1^T & B_0 \\ -C^TZC & -A^T & 0 \\ \hline 0 & B_0^T & 0 \end{array}\right] \tag{24}$$

Using spectral factorization results from Ref. 17, the stable factor of M^*M is

$$M = \left[\begin{array}{c|c} \bar{A} + YC^TZC & B_0 \\ \hline Z^{1/2}C & 0 \end{array}\right] \tag{25}$$

where Y is the stabilizing solution to the Riccati equation (21). Substituting Eq. (23) into Eq. (16), yields that the cost $L(\hat{H}, \gamma)$ is given by $\|M\|_2^2$, where $\|M\|_2^2 = \text{tr}\,\{C^TZCQ\}$ and Q satisfies the Lyapunov equation (22).[18] □

The compensator of a given fixed order that minimizes this cost can be found using a numerical optimization technique. The system can be described by the plant F

$$F \sim \left[\begin{array}{c|ccc} A & B_0 & B_1 & B_2 \\ \hline C_1 & 0 & D_{11} & D_{12} \\ C_2 & D_{20} & D_{21} & D_{22} \end{array}\right] \tag{26}$$

where A has dimension n. The inputs to F are the disturbances corresponding to H_0 and H_1, and the control u, and the outputs are the performance and the sensed output y. For an optimal solution to exist, require that (A, B_2) be stabilizable, (A, C_2) be detectable, $D_{12}^TD_{12} > 0$ and $D_{2i}D_{2i}^T > 0$ for $i = 0, 1$. If the (strictly proper) compensator K, with state-space dimension n_c, is represented as

$$K \sim \left[\begin{array}{c|c} A_c & B_c \\ \hline C_c & 0 \end{array}\right] \tag{27}$$

then the closed-loop system is given by the LFT

$$\hat{H}_{cl} = \mathcal{F}(F, K) \sim \left[\begin{array}{cc|cc} A & B_2C_c & B_0 & B_1 \\ B_cC_2 & A_c + B_cD_{22}C_c & B_cD_{20} & B_cD_{21} \\ \hline C_1 & D_{12}C_c & 0 & D_{11} \end{array}\right] \tag{28}$$

The cost can be evaluated using Theorem 2. The necessary conditions that an optimal compensator must satisfy can be obtained by appending the constraint equations (21) and (22) to the cost in Eq. (20) using matrix Lagrange multipliers X and P, and differentiating the augmented cost with respect to X, Y, P, Q, and the free parameters of the compensator system matrix. Making the appropriate definitions in comparing Eqs. (28) and (18), Y satisfies the Riccati equation (21), Q satisfies the Lyapunov equation (22), P satisfies the dual Lyapunov equation

$$P(\bar{A} + YC^TZC) + (\bar{A} + YC^TZC)^TP + C^TZC = 0 \tag{29}$$

and X satisfies

$$X(\bar{A} + YC^TZC) + (\bar{A} + YC^TZC)^TX + PQC^TZC + C^TZCQP = 0 \tag{30}$$

A similar approach has been used to solve a variety of control problems, e.g., Ref. 19, wherein the necessary conditions are simplified by identifying a projection operator. Here a similar projection operator has not been identified, due to the multiple constraint structure of the problem. Similar multiple-constraint fixed-order problems are investigated in Ref. 20. It appears likely that for this problem, the optimal compensator with no constraint on the compensator state dimension does not have finite order. In practice, the compensator order can be increased until there is no significant decrease in the cost.

The gradients of the augmented cost with respect to the controller parameters are given by

$$\frac{\partial J}{\partial A_c} = (PQ)_{22} + (XY)_{22} \tag{31}$$

$$\begin{aligned} \frac{\partial J}{\partial B_c} &= (P_{12}B_0 + P_{22}B_cD_{20})D_{20}^T \\ &+ \gamma^{-1}(X_{12}B_1 + X_{22}B_cD_{21})WD_{21}^T + \gamma^{-1}([PQ+XY]_{21}C_1^T \\ &+ (PQ+XY)_{22}C_c^TD_{12}^T]ZD_{11}D_{21}^T + (PQ+XY)_{21}C_2^T \\ &+ (PQ+XY)_{22}C_c^TD_{22}^T \end{aligned} \tag{32}$$

$$\frac{\partial J}{\partial C_c} = D_{12}^T Z [C_1 (Q + QPY + YPQ + YXY)_{12} + D_{12} C_c (Q + QPY + YPQ + YXY)_{22}] + \gamma^{-2} D_{12}^T Z D_{11} [B_1^T (PQ + XY)_{12} + D_{21}^T B_c^T (PQ + XY)_{22}] + B_2^T (PQ + XY)_{12} + D_{22}^T B_c^T (PQ + XY)_{22} \quad (33)$$

where the implied partitioning of the $(n + n_c) \times (n + n_c)$ matrices P, Q, X, and Y and their products is into $n \times n$, $n \times n_c$, $n_c \times n$ and $n_c \times n_c$ blocks.

Several comments about the numerical algorithm can be made. First, $\gamma > 1$ for any structure, and because a strictly proper compensator cannot dissipate power as $\omega \to \infty$, the cost is only well defined for $\gamma > 1$. However, the compensator is only guaranteed to be positive real for $\gamma \leq 1$. Rather than relying on knowledge of the damping, the parameter γ should be set close to unity. Second, any positive real compensator is guaranteed to stabilize the structure and hence satisfy the $\mathcal{H}_\infty$-norm constraint. However, since the optimization problem is nonconvex, local minima are likely to exist, and thus an initial guess that is close to the expected optimum is desirable. Herein, the $\mathcal{H}_\infty$ impedance matching solutions of Ref. 7 were used. Next, note that the representation of the compensator in Eq. (27) contains $n_c \times (n_c - 1)$ extra degrees of freedom, since the state-space representation is only unique to within a similarity transformation. However, constraining the form of the compensator further is likely to introduce more local minima, and does not necessarily lead to a faster optimization.[11] In practice, A_c was constrained to be tridiagonal. Finally, note that $H_0 = WH_1$ for some weighting function W. Hence, the Riccati equation for Y only needs to be solved for a system with state dimension equal to that of H_1. Furthermore, since the states of W are uncontrollable from B_2, the system matrix in Eq. (28) can be written in upper block triangular form, and the Lyapunov equations for Q, P, and X can be solved more efficiently by taking advantage of this structure.

V. Experimental Verification

The approach described in the previous sections was tested on the multipoint alignment testbed in the Space Engineering Research Center laboratory at the Massachusetts Institute of Technology. This testbed and the associated research program are intended to evaluate the benefits of the application of controlled structures technology to a space-based astronomical interferometer requiring large baselines and precision alignment. A detailed description of the testbed, its scientific motivation, performance metric, disturbances, sensors, and actuators can be found in Ref. 21. The following section gives a brief synopsis of the relevant details.

A. Interferometer Testbed Description

The interferometer testbed is a 1/10 scale model of the space-based mission. Six 3.5-meter-long triangular truss legs form a tetrahedron, as shown schematically in Fig. 4 (from Ref. 21). Three mock siderostats, labeled A, B, and C, are located on three legs of the truss. Light from the science star would be collected by these siderostats and combined at the vertex labeled F. The phase difference between these light waves determines information about the science star. A laser is mounted at vertex F to provide an optical measurement of the pathlength between this vertex and each of the three siderostat locations. The difference between each pair of pathlengths will be denoted $A-B$, $B-C$, and $C-A$. To measure the relative phase of light from different siderostats, each possible differential pathlength (DPL) must be reduced to below 50 nm rms displacement between 10 and 500 Hz. The disturbance environment is created by three piezoelectric disturbance sources mounted at the vertex labeled G. The force spectrum for these actuators is not that specified in Ref. 21, but is instead flat at low frequencies, with a two-pole roll-off at 70 Hz.

The contribution to the open-loop DPL in different frequency regimes is shown in Fig. 9. On average, for the three different differential pathlengths, over 85% of the mean-square displacement occurs above 80 Hz. The current finite element model of the structure does not accurately predict the modal frequencies or mode shapes above 80 Hz. Thus any active control for this frequency region must either be based on a measurement model or use an approach that does not rely on precise knowledge of the modal frequencies.

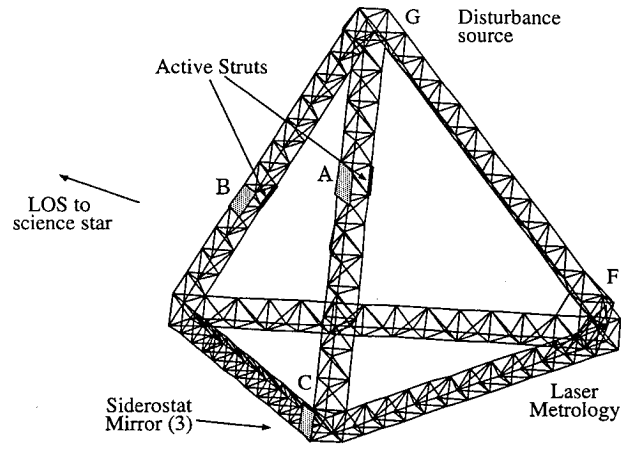

Fig. 4 Definition of geometry for testbed performance metric.

Since the goal of low authority control is to add active damping, the active approach can also be compared with a passive damping approach. A high loss factor viscous "D-strut" was used,[22] which can be interchanged with any strut on the structure. Each strut has a stiffness comparable to the dynamic stiffness of the structure at 50 Hz, and a peak loss factor between $\eta = 1$ and $\eta = 1.5$, which occurs between 55 and 70 Hz. These struts are designed to add significant damping in a frequency range that is relatively narrow compared with the damping provided by a viscoelastic treatment. This frequency distribution for the damping is consistent with the goals of low authority control. The damping requirements of the LAC are broadband relative to those of an HAC, in the sense that authority is desired over a large number of modes. However, the requirements on the LAC are often narrowband relative to the damping provided by constant gain (or rate) feedback.

B. Control System Design

Active struts actuators were used, which can replace any single strut on the interferometer truss, giving the control designer a great deal of flexibility in placement. Each active strut contains a preloaded piezoceramic stack and a load cell. Two active struts were sufficient to demonstrate the effectiveness of the control design techniques, although more would be necessary to demonstrate substantial performance improvements. The two low authority control laws can be designed and implemented independently. Because the LAC relies on phase stabilization, the compensator must remain positive real at frequencies much higher than that at which performance is desired. Thus, without a very high sample rate, the time delay of a digital computer is unacceptable, and analog circuits were used instead.

To get sufficient control authority over those modes that strongly influence the performance metric, the active struts were placed in the truss longerons opposite the siderostat plates A and B in Fig. 5. Note that placement schemes based on maximum residue locations of the finite element model are inconsistent with the assumptions of poor modal information that require low authority control.

The load cell in the active strut can be considered to be collocated with the actuator, since the frequency at which noncollocation becomes important is much higher than required. However, for impedance matching control, the actuated and sensed variable should also be dual, in the sense that their product should be the power flow into the structure. In general, the piezoelectric actuator provides neither pure force nor pure displacement. In the interferometer testbed, however, the active strut is significantly stiffer

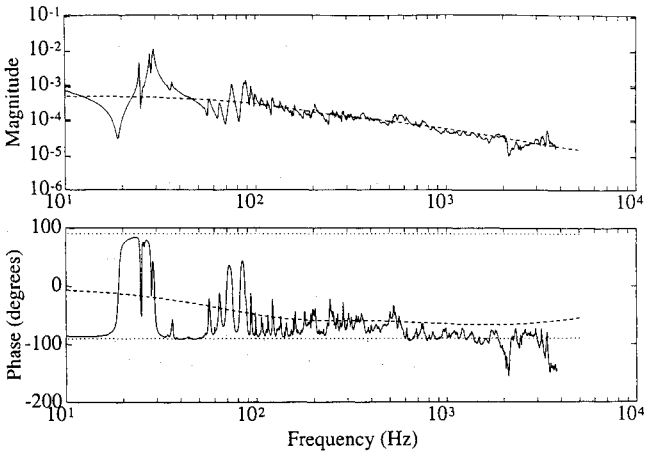

Fig. 5 Measured (solid) and dereverberated (dashed) transfer function between active strut voltage and integrated force near plate *B*.

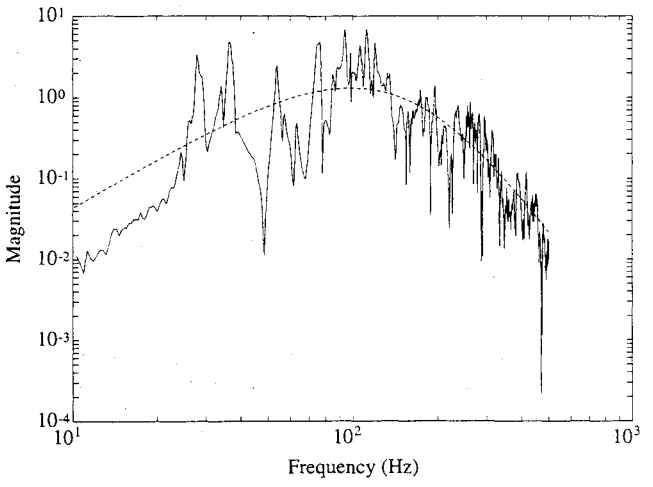

Fig. 6 Weighting function used in control design (dashed) and transfer function from disturbance to pathlength *BF* (solid).

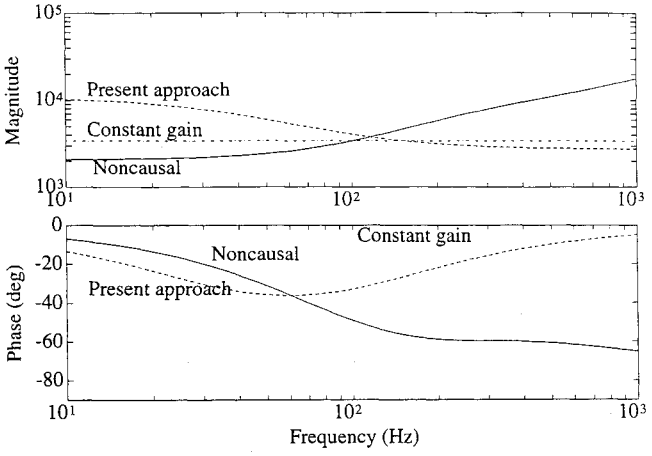

Fig. 7 Compensators for active strut at plate *B*: noncausal optimum (solid), constant gain solution (dash-dot), and present approach (dashed).

than the dynamic stiffness of the rest of the structure in the frequency range of interest, and it therefore commands displacement. It also effectively commands the extension rate of the strut, and the dual variable to extension rate is force. Thus, the impedance matching solution requires that the extension rate and force be related through a compensator, or equivalently, that the extension and the integral of force be related. Integral of force feedback has been used elsewhere for stiff actuators (see, e.g., Ref. 23).

To design impedance matching compensators between the integral of force and the stack voltage, the dereverberated driving point transfer function must be identified. As noted in Sec. II, this transfer function can be determined by averaging the log magnitude of the experimental transfer function. For both of the active strut transfer functions, three poles were found to be adequate to describe the dereverberated transfer function in the frequency range of interest. The fitted and measured transfer functions are plotted for the active strut at plate *B* in Fig. 5. The measured transfer functions at *A* and *B* are positive real up to 622 Hz, and are within 10 deg of positivity up to 1500 Hz, where the dynamics of the actuator and sensor, or the noncollocation, becomes important. The plotted transfer function also assumes perfect integration. The load cell integrator was rolled off at low frequencies with a corner frequency of $\omega_i = 11.25$ Hz and a damping ratio of $\zeta_i = 0.7071$, to prevent saturation, and this determines a low frequency limit to positivity as well.

Once the dereverberated transfer function has been identified, various compensators can be designed. The compensator that dissipates the maximum power from a structure is the impedance match given by Eq. (4). This optimization yields a noncausal transfer function, which cannot be implemented, and must be approximated.

The simplest approximation that can be made is to constrain the compensator to be a constant gain. The optimal gain at a given frequency ω_0 can easily be shown to be the magnitude of the noncausal solution at that frequency, so that

$$K_C = \frac{1}{|G(j\omega_0)|} \tag{34}$$

This is the "rate feedback" solution. The constant gain solution only corresponds to feedback of rate for a force actuator. For any other actuator, constant gain impedance matching generalizes the concept of rate feedback.

Now consider the design of compensators using the technique developed in Secs. III and IV. If a low authority controller is required only to provide robustness for a high authority compensator, then the weighting function $C(\omega)\Pi_{in}(\omega)$ in Eq. (14) is specified by the requirements of the HAC. However, in the case of the interferometer testbed, the bandwidth of the disturbance and performance specification, combined with the errors in the model, require that the low authority controller provide a direct performance benefit. The frequency distribution of the active damping requirements are dictated by the disturbance input power and the performance. The product $C(\omega)\Pi_{in}(\omega)$ can be determined by fitting the measured transfer function from disturbance to performance with real poles and zeroes. The resulting seven pole weighting function $W(j\omega)$ is shown in Fig. 6. The filter that shapes the spectrum of the disturbance is included in the transfer function. The central frequency ω_0 in the constant gain feedback, Eq. (34), was chosen to be 100 Hz, where this weighting function is a maximum.

For both strut locations, the optimal compensators corresponding to the chosen weighting require only a single pole-zero pair. Increasing the compensator order further did not appreciably change the cost. The resulting compensators are shown in Fig. 7 for the strut at siderostat plate *B*. Those for the active strut at plate *A* are similar. Greater damping is obtained by the frequency dependent compensators by more closely matching both the magnitude and phase of the noncausal optimum at the center frequency of the weighting function. The closed-loop power reflection coefficient *H* for each of the compensators is plotted in Fig. 8. A value of unity indicates that all of the incoming power is being reflected (no dissipation), whereas a value of zero indicates the "complete" dissipation attained by the ideal noncausal impedance match at that frequency. Although the constant gain compensator was chosen to maximize dissipation at $\omega_0 = 100$ Hz, it achieves its best damping at lower frequencies due to the fact that the experimentally determined dereverberated impedance is almost constant at low fre-

quencies, and thus any constant gain feedback has the correct phase in this frequency region.

C. Results

The performance is composed of the rms differential pathlength error for the three different combinations of pathlengths. This data is shown in Table 1 for several different cases, and by frequency region in Fig. 9 for pathlength *B–C*. The baseline testbed configuration has no active or passive damping struts in place. Adding the active struts to the structure, with no control, results in a change in the performance metric due to the different stiffness and damping characteristics of the active strut as compared to a nominal strut. The performance with each active strut replaced by a D-strut is included to illustrate the possible improvement in damping achieved per strut by an active technique over a passive technique. Finally, active control using the optimization approach of this paper yields about a 30% increase in the performance achieved per strut over the constant gain solution.

Several observations about the performance can be made. Below the first mode of the structure, the dereverberated model is not valid, and the feedback destiffens the active strut. The resulting increase in the displacement autospectrum is more than offset by the decreases at higher frequencies. Second, as predicted by the power flow analysis in Fig. 8, the approach of this paper achieves greater damping in the frequency region around 100 Hz than the constant gain feedback. Finally, note that in this experiment, only 2 of the 641 struts in the structure were actively damped. The purpose of the experiment was not to demonstrate the performance achievable by LAC, but rather to compare alternative LAC techniques. A larger number of active struts would be required to achieve substantial performance improvements.

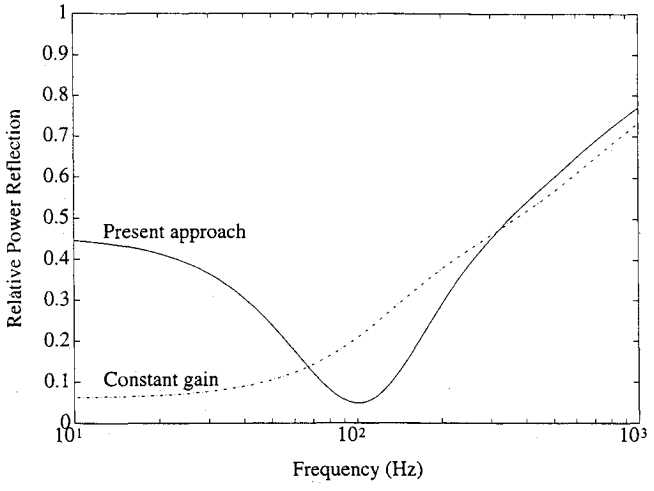

Fig. 8 Relative power dissipation for compensators at plate *B*: constant gain solution (dash-dot) and present approach (solid).

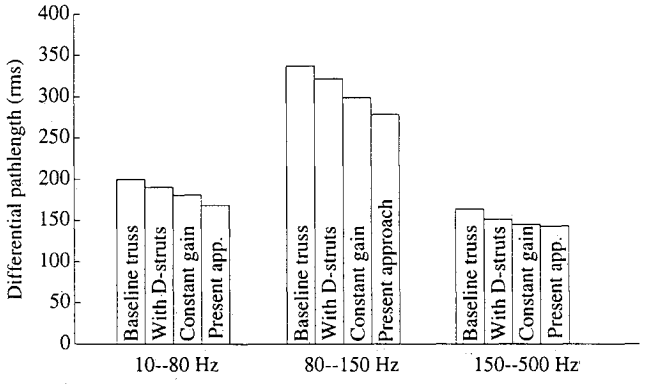

Fig. 9 Differential pathlength error *B–C*, for baseline, with two D-struts, with constant gain feedback, and using the present approach (rms in nm).

Table 1 Achieved performance and relative change with respect to baseline for 10–500 Hz

	rms DPL in nm			% change		
	A–B	*B–C*	*C–A*	*A–B*	*B–C*	*C–A*
Baseline truss	495	417	602	0	0	0
With active struts	492	424	594	–0.7	1.8	–1.2
With D-struts	469	403	564	–5.4	–3.3	–6.2
Constant gain	443	378	557	–10.5	–9.4	–7.4
Present approach	444	355	549	–10.4	–14.9	–8.8

The data presented earlier gives the improvement in performance obtained by using low authority control alone. However, another benefit of implementing a LAC is that it adds damping in the roll-off region of a high authority control loop. As a result, higher performance HAC controllers can be implemented. Therefore, the performance improvement that can be attributed to low authority control also includes the difference between the achievable performance of a high authority controller before and after implementation of the LAC.

Note that if broadband damping is required, a passive damping scheme might incur a smaller weight penalty than an active approach. However, most applications will have relatively narrowband requirements on the added damping. This is the case for the performance specifications of the interferometer problem, or for the requirement of adding damping in the roll-off region of a high authority controller. In these cases, an active approach has advantages over passive damping augmentation. This result is due to the greater peak damping capability of an active approach, together with its flexibility in tuning the target frequency, and the potential elimination of any weight penalty by using the same hardware as the HAC.

VI. Conclusions

A structural modeling approach based on the modeling principles of statistical energy analysis can be used to represent the average value of a global mean-square performance metric in terms of only local structural information. The local information is given by the experimentally determined dereverberated transfer function. The approach yields a mixed $\mathcal{H}_2/\mathcal{H}_\infty$ optimization problem, which can be solved numerically. The resulting optimal compensators guarantee closed-loop stability. The approach was tested on a complex laboratory structure, and approximately 30% better performance reduction was obtained over the usual rate feedback, or constant gain, approach. The active approach achieved greater performance reduction than a passive approach due to a higher peak damping capability and the ability to tune the controller to target the most important frequency region.

Acknowledgments

The research was supported by Sandia National Laboratory under Contract 69-4391 and by the Massachusetts Institute of Technology Space Engineering Research Center (SERC) under NASA Grant NAGW-1335. The suggestions of Dennis Bernstein, Andreas von Flotow, and David Miller are appreciated, as is the assistance of Dina Pery and the rest of the SERC interferometer team.

References

[1]Balas, M. J., "Trends in Large Space Structure Control Theory: Fondest Hopes, Wildest Dreams," *IEEE Transactions on Automatic Control*, Vol. AC-27, No. 3, 1982, pp. 522–535.

[2]Lyon, R. H., *Machinery Noise and Diagnostics*, Butterworth Publishing, Boston, June 1987.

[3]Aubrun, J.-N., "Theory of the Control of Structures by Low-Authority Controllers," *Journal of Guidance and Control*, Vol. 3, No. 5, 1980, pp. 444–451.

[4]Hodges, C. H., and Woodhouse, J., "Theories of Noise and Vibration Transmission in Complex Structures," *Reports on Progress in Physics*, Vol. 49, 1986, pp. 107–170.

[5]Lyon, R., *Statistical Energy Analysis of Dynamical Systems: Theory and Applications*, The MIT Press, Cambridge, MA, 1975.

[6]Hall, S. R., MacMartin, D. G., and Bernstein, D. S., "Covariance Averaging in the Analysis of Uncertain Systems," *IEEE Transactions on Automatic Control*, Vol. 38, No. 12, 1993, pp. 1858–1862.

[7]MacMartin, D. G., and Hall, S. R., "Control of Uncertain Structures using an $\mathcal{H}_\infty$ Power Flow Approach," *Journal of Guidance, Control, and Dynamics*, Vol. 14, No. 3, 1991, pp. 521–530.

[8]von Flotow, A. H., and Schäfer, B., "Wave-Absorbing Controllers for a Flexible Beam," *Journal of Guidance, Control, and Dynamics*, Vol. 9, No. 6, 1986, pp. 673–680.

[9]Miller, D. W., Hall, S. R., and von Flotow, A. H., "Optimal Control of Power Flow at Structural Junctions," *Journal of Sound and Vibration*, Vol. 140, No. 3, 1990, pp. 475–497.

[10]Skudrzyk, E., "The Mean-value Method of Predicting the Dynamic Response of Complex Vibrators," *Journal of the Acoustical Society of America*, Vol. 67, No. 4, 1980, pp. 1105–1135.

[11]MacMartin, D. G., "A Stochastic Approach to Broadband Control of Parametrically Uncertain Structures," Ph.D. Dissertation, Dept. of Aeronautics and Astronautics, Massachusetts Institute of Technology, Cambridge, MA, June 1992.

[12]Lyon, R. H., "Statistical Analysis of Power Injection and Response in Structures and Rooms," *Journal of the Acoustical Society of America*, Vol. 45, No. 3, 1969, pp. 545–565.

[13]Nelson, P. A., Curtis, A. R. D., Elliot, S. J., and Bullmore, A. J., "The Active Minimization of Harmonic Enclosed Sound Fields, Part I: Theory," *Journal of Sound and Vibration*, Vol. 117, No. 1, 1987, pp. 1–13.

[14] Zhou, K., Doyle, J., Glover, K., and Bodenheimer, B., "Mixed $\mathcal{H}_2$ and $\mathcal{H}_\infty$ Control," *Proceedings of the American Control Conference* (San Diego, CA), May 1990, pp. 2502–2507; also *IEEE Transactions on Automatic Control* (to be published).

[15]MacMartin, D. G., Hall, S. R., and Mustafa, D., "On a Cost Functional for $\mathcal{H}_2$ and $\mathcal{H}_\infty$ Minimization," *Proceedings of the 29th IEEE Conference on Decision and Control* (Honolulu, HI), Dec. 1990, pp. 1010–1012.

[16] Boyd, S. P., and Barratt, C. H., *Linear Controller Design: Limits of Performance*, Prentice-Hall, Englewood Cliffs, NJ, 1991.

[17]Francis, B. A., *A Course in $\mathcal{H}_\infty$ Control Theory*, Springer-Verlag, Berlin, 1987.

[18]Doyle, J. C., Glover, K., Khargonekar, P. P., and Francis, B. A., "State-Space Solutions to Standard $\mathcal{H}_2$ and $\mathcal{H}_\infty$ Control Problems," *IEEE Transactions on Automatic Control*, Vol. AC-34, No. 8, 1989, pp. 831–847.

[19]Bernstein, D. S., and Hyland, D. C., "The Optimal Projection Approach to Robust, Fixed-Structure Control Design," *Mechanics and Control of Space Structures*, edited by J. L. Junkins, AIAA, Washington, D. C., 1990, pp. 237–293.

[20]MacMartin, D. G., Hall, S. R., and Bernstein, D. S., "Fixed Order Multi-Model Estimation and Control," *Proceedings of the American Control Conference* (Boston, MA), June 1991, pp. 2113–2118.

[21]Blackwood, G. H., Jacques, R. N., and Miller, D. W., "The MIT Multipoint Alignment Testbed: Technology Development for Optical Interferometry," *Proceedings of the SPIE Conference on Active and Adaptive Optical Systems* (San Diego, CA), July 1991 (SPIE 1542-34).

[22]Anderson, E., Trubert, M., Fanson, J., and Davis, L., "Testing and Application of a Viscous Passive Damper for Use in Precision Truss Structures," *Proceedings of the AIAA Structures, Structural Dynamics, and Materials Conference* (Baltimore, MD), AIAA, Washington, DC, 1991, pp. 2796–2808 (AIAA Paper 91-0996).

[23]Preumont, A., Dufour, J.-P., and Malékian, C., "Active Damping by a Local Force Feedback with Piezoelectric Actuators," *Journal of Guidance, Control, and Dynamics*, Vol. 15, No. 2, 1992, pp. 390–395.